Testing and analysis of the impact on engine cycle parameters and control system modifications using hydrogen or methane as fuel in an industrial gas turbine

H. H.-W. Funke J. Keinz* S. Börner* P. Hendrick** R. Elsing****

**Aachen University of Applied Sciences*
Hohenstaufenallee 6, 52064 Aachen, Germany

***Université Libre de Bruxelles*
Avenue F.D. Roosevelt 50, 1050 Bruxelles, Belgium

****Diehl Aerospace GmbH*
Alte Nußdorfer Str. 23, 88642 Überlingen

Abstract

The paper highlights the modification of the engine control software of the hydrogen converted gas turbine APU GTCP 36-300 allowing safe and accurate methane operation achieved without mechanical changes of the metering unit. The acceleration and deceleration characteristics of the engine controller from idle to maximum load are analysed comparing hydrogen and methane. The paper also presents the influences on the thermodynamic cycle of the gas turbine resulting from the different fuels supported by a gas turbine cycle simulation for hydrogen and methane using the software GasTurb.

1. Introduction

Aviation and power generation industry has need of efficient, reliable, safe and low-pollution energy conversion systems in the future. Therefore, gas turbines will play a decisive role in long-term high power application scenarios. Due to the finite resources of fossil fuels, hydrogen, hydrogen-rich synthesis gases and natural gas with high methane ratios have great potential as renewable and sustainable energy sources derived from wind- or solar power and gasification of biomass substituting fossil energy [1].

Operating a common industrial gas turbine with such alternative fuels, some important major impacts on the system gas turbine have to be considered carefully. For instance, hydrogen has a high reactivity requiring combustion chamber modifications to guarantee efficient, stable and safe combustion. In addition, low NO_x combustion becomes an important environmental related issue. Besides combustion technology and related exhaust gas emissions, modifications of the gas turbine control and fuel metering system have to be applied to guarantee safe, rapid and precise changes of the engine power settings [2][3][4][5][6][7]. Against this background the Gas Turbine Section of the Department of Aerospace Engineering at Aachen University of Applied Sciences works in the research field of low-emission combustion chamber technologies for hydrogen gas turbines and related topics and investigates the complete system integration of combustion chamber, fuel system, engine control software and emission reduction technologies. Besides hydrogen, in the current scope of research hydrogen-rich synthesis gases and methane as future green and sustainable gas turbine fuels produced by renewables are in the focus.

In order to demonstrate the conversion abilities of gas turbines from kerosene to gaseous alternative fuels, this paper presents the modification of a formerly kerosene-driven hydrogen gas turbine for methane operation. The objective regarding the aspect of engine control is to maintain the operational characteristic of the kerosene gas turbine using hydrogen and methane without performing major modifications on the gas turbine structural and control architecture. The transition from kerosene to hydrogen, i.e. from a liquid to a gaseous fuel, has an important impact on the chosen control and fuel metering strategy of the gas turbine. The further application to methane only requires minor changes at the engine controller and the metering unit without any mechanical changes to the gas turbine.

2. Experimental Gas Turbine Test Rig APU GTCP 36-300

Investigating the feasibility of alternative fuels such as hydrogen, hydrogen-rich synthesis gases and methane in gas turbine engines and their impact on engine control strategy, an aircraft Auxiliary Power Unit (APU) GTCP 36-300 is used as experimental test rig at Aachen University of Applied Sciences (Figure 1).

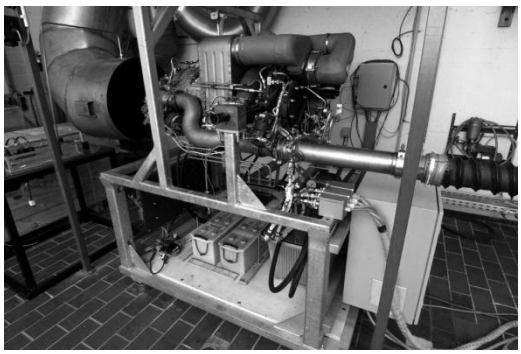

Figure 1: APU GTCP 36-300 on test rig

The GTCP 36-300 is a single spool gas turbine engine with a single-stage radial compressor and a single-stage radial turbine requiring about 1.6 MW thermal energy converted to shaft power for production of electrical and pneumatic power up to 335 kW provided by an auxiliary generator and an additional single-stage radial load compressor controlled by the Versatile Engine Control Box (VECB) built by Diehl Aerospace GmbH. The combustion section consists of an annular reverse flow combustion chamber with six circumferentially distributed fuel nozzles. The APU is modified for operation from liquid kerosene to gaseous hydrogen and methane by replacing the genuine kerosene fuel nozzles with six nozzles for gaseous fuels, by implementing a metering unit for gaseous fuels and by installing a hydraulic system to perform hydraulic functions which were previously achieved also with kerosene as hydraulic medium.
The APU 36-300 has several load modes depending on the required electric or pneumatic demand in the aircraft. These modes can be separated into two main modes. First there is the Environmental Control Supply (ECS) mode where the APU delivers compressed air for the aircraft air conditioning system and which can be adjusted in stages to several load conditions from idle to maximum ECS load. All ECS stages operate at constant rotational speed of 99% while the power output is controlled by movable Inlet Guide Vanes (IGV) which open or close depending on the particular power demands. Additionally, there is the Main Engine Start (MES) mode delivering the maximum electric and pneumatic power output of the APU required for the start procedure of the aircraft main engines; this mode runs on a constant rotational speed of 101%.
The GTCP 36-300 is a rotational speed controlled gas turbine engine and the conversion of the APU from kerosene to hydrogen and furthermore to methane bases on the concept of feeding the same requested amount of thermal heat into the combustion chamber regardless which fuel is used, achieving similar gas turbine operation characteristics for all modes of operation by maintaining the designated rotational speed for each load condition. In [4], [5], [6] and [7] the successful implementation of a metering unit for gaseous fuels (Figure 2), the modification of the fuel control system and the re-programming of the VECB (engine controller) for the use of hydrogen instead of kerosene are described. Reference [5] shows the start-up and acceleration behaviour of the APU with hydrogen.
Based on this experience, the paper presents the successful conversion of the APU from gaseous hydrogen to gaseous methane and the control behaviour at different loads, its acceleration and deceleration behaviour with the installed nozzles for gaseous fuels without modifications of the fuel nozzles or any changes of the gas turbine mechanical structure or the combustion chamber.

3. Conversion of the APU GTCP 36-300 from Hydrogen to Methane

3.1 Adaption of the Gas Turbine Fuel Metering and Control

Hydrogen and methane have very different properties, e.g. heating value, air requirement, flammability range and flame speed. Therefore, the change from hydrogen to methane has an impact on the combustion characteristics and the thermodynamic gas turbine cycle (ref. to chapter 4) influencing the engine control behaviour. Comparing hydrogen and methane, the lower heating value *LHV* of hydrogen is much higher. The same trend is valid for the stoichiometric air requirement *SAR* while methane does not differ from kerosene in a great extent (ref. to Table 2).

As a consequence two philosophies are possible when converting a kerosene-APU to hydrogen and methane. (i) Because of its properties, hydrogen would have a lower combustion temperature than kerosene when equal heat flow rates are maintained, resulting in an increase in turbine hot parts lifetime, because the thermal load on these parts would be decreased. (ii) This leads to the converse argument that when the hydrogen operation is scaled to meet the same turbine inlet temperature or exhaust gas temperature as with kerosene considering the temperature limits of the turbine hot parts, the gas turbine power can be increased subsequently. The same applies for methane, but in a minor extend. In the current scope of work the first approach is chosen.
Regarding the flammability range of the fuels, hydrogen and methane are also much different. Hydrogen is flammable in the range of 4-75 Vol.% in air [8]. The flammability of methane is ensured only between 4.4-15 Vol.% in air [9] posing a challenge in the fuel metering and control adaption at the gas turbine start-up. As described in [6] the APU GTCP 36-300 modified for the operation with hydrogen is controlled by the genuine Versatile Engine Control Box (VECB) from Diehl Aerospace which was formerly designed for kerosene and is now adapted to the use of gaseous fuels only by software modifications. These modifications enabled the original engine controller to control both the gas turbine and the metering unit for gaseous fuels by implementing an additional control loop for the metering unit. This avoids the need of additional and separate controller equipment for the metering unit when using gaseous fuels.

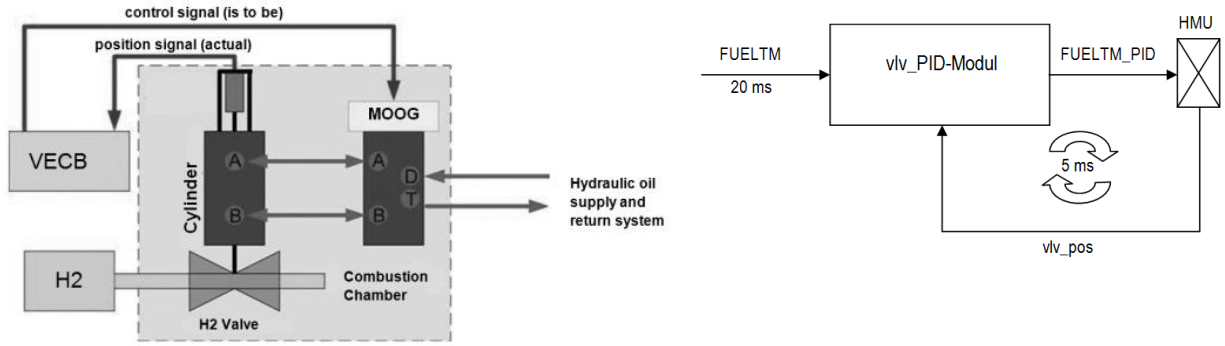

Figure 2: Metering unit for gaseous fuels (left) and implemented metering unit control loop (right) [5]

In Figure 2 the set-up of the metering unit and the additional control loop are illustrated. Every 20 milliseconds the main engine controller sends the requested fuel flow (FUELTM) to the implemented metering unit controller (vlv-PID-Modul). Each amount of fuel is assigned a certain valve opening position. The metering unit controller sends a control current (FUELTM_PID) to the metering unit MOOG-valve at the metering unit (HMU). The vlv_PID-Modul-controller operates the hydraulic MOOG valve with a clocking of 5 milliseconds. By operating the MOOG valve the hydraulic cylinder traverses the hydrogen fuel valve to the requested position. The actual position of the fuel valve (vlv_pos) is measured by a positioning encoder and reported back to the controller. Besides the implementation of the additional control loop, security laws for the application of hydrogen are implemented [6] and are maintained for methane operation.
The gas turbine operation is controlled by the main engine controller working according to two different philosophies: during the ignition and the starting sequence, i.e. from 0% to 95% rotational speed, the engine is controlled by the start-up-controller. At 95% a second controller, also referred to as on-speed-governor, takes over. The on-speed-governor controls the engine operational behaviour and keeps the rotational speed constant depending on the selected mode: 99% speed for all ECS load stages and 101% speed for MES. The on-speed-governor controls the rotational speed to the constant value according to ECS or MES independent from the selected load stage by varying the fuel quantity. While the behaviour of the on-speed-governor is the same in kerosene, hydrogen and methane operation, the acceleration controller is to be modified for the methane operation.
According to the different properties of hydrogen and methane it is necessary to first determine the required fuel mass flow of methane under the premise of an equal thermal heat flow rate in the combustion chamber for both fuels:

$$\dot{Q}_{CH_4} = \dot{Q}_{H_2} \tag{1}$$

This basic layout criterion leads to the relation for the calculation of the required fuel mass flow for methane, which happens to be 2.4 times higher than the required fuel mass flow of hydrogen (also ref. to Table 2) what will certainly have an influence on the controller behaviour:

$$\dot{m}_{CH_4} = \dot{m}_{H_2} \cdot \frac{LHV_{H_2}}{LHV_{CH_4}} = \dot{m}_{H_2} \cdot \frac{119.95}{50.03} = 2.4\ \dot{m}_{H_2} \tag{2}$$

The start-up-controller uses a function of speed for the metering during the starting process. A valve opening position and therewith a defined fuel flow is attributed to several decided speed steps during the acceleration of the gas turbine up to 95% rotational speed. Between two speed steps the controller interpolates the valve opening position [5]. According to the different required fuel flow with methane the speed step FUELTM values of hydrogen implemented in the controller must be transferred into FUELTM values for the methane acceleration process considering equal heat flow rates. To account for the reduced *LHV* of methane the initial control current FUELTM_PID in the control loop is increased to assure a high enough amount of fuel at speeds below 30% for the initial acceleration (fuel spiking). In addition, the initial speed step in the start-up controller is shifted to an earlier rotational speed to ensure safe ignition at the start-up procedure with increased fuel flow considering the heating value and the narrow flammability limits of methane. With these minor modifications in the start-up-controller the acceleration process can be realized without difficulties and the controller changeover from the start-up-controller to the on-speed-governor at 95% rotational speed also is ensured, so the gas turbine accelerates to 99% constant rotational idle speed. At the on-speed-governor no modifications of the PID-parameters are performed and the same PID-parameters from hydrogen operation are maintained. In [5] and [7] the ignition and acceleration characteristics of the hydrogen operating APU GTCP 36-300 are described in detail for comparison.

3.2 Engine Operational Behaviour at Acceleration Idle-MES and Deceleration MES-Idle

After establishing stable and secure idle operation of the gas turbine, especially the acceleration and deceleration characteristics of the engine controller behaviour from idle to maximum load operation mode MES comparing hydrogen and methane are of interest. Figure 3 shows the measured results of the rotational speed and setting of the MES load condition by means of the IGV position during the acceleration from idle to MES and the deceleration from MES back to idle. The rotational speed is depicted on the left axis in per cent of the maximum speed; the IGV position is described as the guide vane angle in degree on the right axis; on the abscissa the time is applied by means of a dimensionless time index.

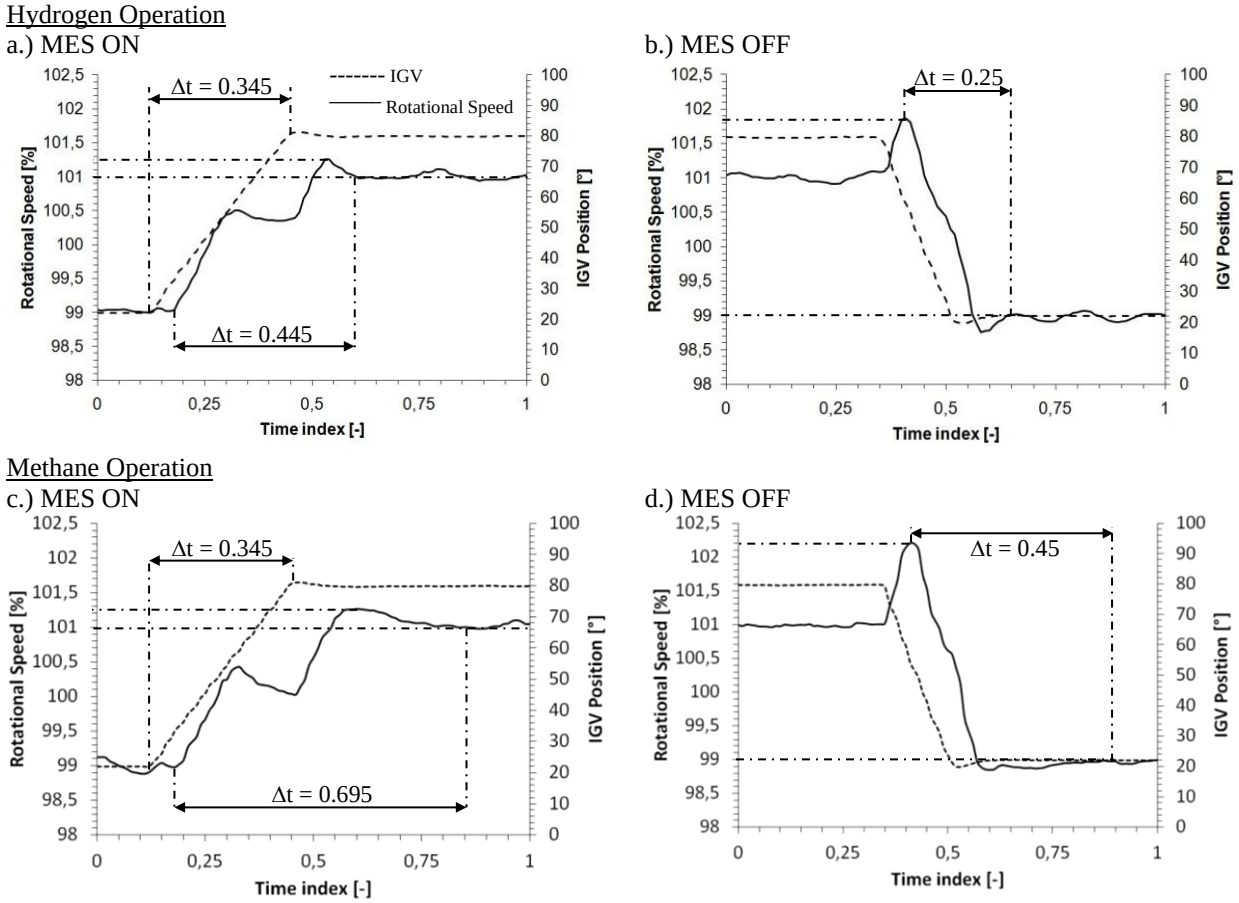

Figure 3: Acceleration and deceleration behaviour of the engine controller for MES of hydrogen and methane

The load change to MES is initiated by switching the IGV position from about 20° to 80° with a simultaneous boost in the rotational speed from 99% to 101% to increase the bleed air flow in the pneumatic system for the main engine start procedure. It can be observed that the adjustment of the IGV angle for either the acceleration or the deceleration process is identical for both hydrogen and methane operation which results in a comparable load change. For the adjustment of the rotational speed a different effect is observed. Regarding the change from idle to MES the on-speed-governor controls the rotational speed to 101% for both fuels after a slight overshoot. While the setting of constant 101% speed is rather fast for hydrogen, the controller takes longer to establish 101% speed when using methane as fuel.
Analysing the change from MES back to idle a similar effect is observed. Again the adjustment time for the IGV positioning is the same for both fuels. When the deceleration process is initiated by the sudden switch-off of the load, the rotational speed at hydrogen operation overshoots to 101.85%; the speed in methane operation overshoots even to 102.20%. After a short time delay in the controller the speed is readjusting to constant 99% idle; in methane operation the time delay again is bigger than in hydrogen operation.
The reason of the differing behaviour in acceleration and deceleration of methane and hydrogen is found when analysing the moving characteristics of the fuel valve at the metering unit for gaseous fuels in Figure 4, where the relative way of opening and closing of the fuel valve each for hydrogen and methane is depicted versus the same time index scaling as in Figure 3.

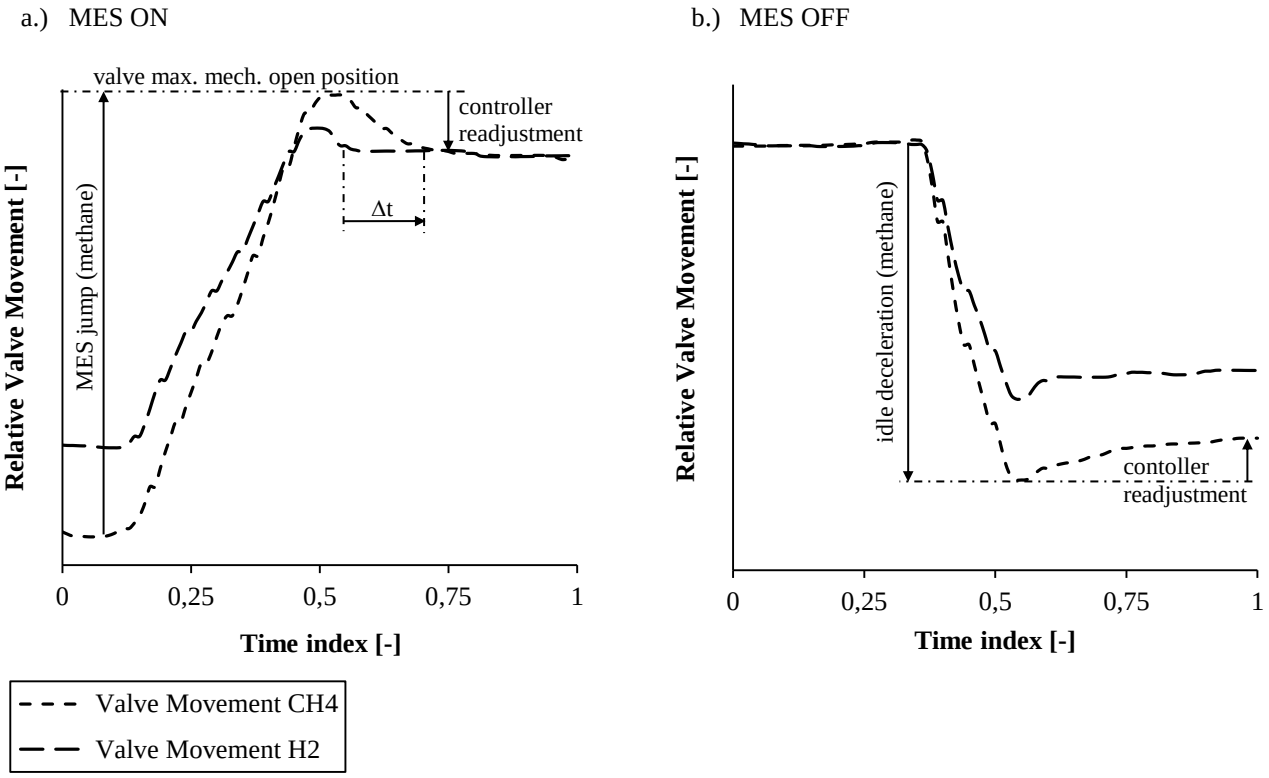

Figure 4: Metering unit fuel valve movement during acceleration (a.) and deceleration (b.)

In Figure 4(a) the relative fuel valve opening at the acceleration from 99% idle to 101% MES is shown. While the traverse path of the valve is relatively small for hydrogen, the on-speed-governor opens the valve much wider for methane when MES mode is initiated with the applied controller settings similar to hydrogen. This initial opening command from the on-speed-governor moves the valve very fast up into its maximum mechanical opening position. A similar effect is due for the deceleration in Figure 4(b). The on-speed-governor initiates the valve closing according to the implemented and maintained control parameters from hydrogen. Again the adjustment is very fast and too excessive and the valve is closed in a much greater extend as required to reach idle forcing the governor to readjust back to the required methane flow.
Despite these small differences, always and with either fuel the acceleration and deceleration of the gas turbine load change is completed safely and reliably. In fact, it can be stated that with minor differences in the controller behaviour between hydrogen and methane the same control settings with slight modifications in the start-up-process and the common metering unit architecture enable a successful starting sequence and operation of the gas turbine with both hydrogen and methane. The engine controller is able to safely and reliably initiate load changes and shows acceptable performance in a dual-fuel hydrogen/methane gas turbine application.

4. Analysis of Gas Turbine Thermodynamic Cycle with Hydrogen and Methane

4.1 APU Performance Model

A change of fuel influences the thermodynamic cycle of the gas turbine [10], [11]. Besides starting procedure and control of the gas turbine, inter alia

- the fuel mass flow,
- the equivalence ratio,
- combustion and turbine inlet temperature,
- the compressor pressure ratio and thereby the characteristics of compressor and turbine
- and the exhaust gas temperature

are influenced. In this section of the paper the presented experimental investigation is completed by a theoretical analysis of the thermodynamic cycle supported by a gas turbine cycle simulation using the software GasTurb [15] for hydrogen and methane. The performance model of the APU GTCP 36-300 in GasTurb is created by regarding the creation of a performance model of a gas turbine from [12], the adjustment of component maps for performance calculations [13] and the correction of model based gas turbine parameters [14]. The applied performance model of the actual APU GTCP 36-300 as it is used at Aachen University of Applied Sciences is already validated against detailed experimental performance test data of the APU manufacturer for kerosene operation. This existing performance model is used as basis to analyse the impact on the thermodynamic cycle of the APU fuelled with hydrogen and methane. The used nomenclature in the following sections to describe some effects is similar to the gas turbine station description from GasTurb shown in Figure 5.

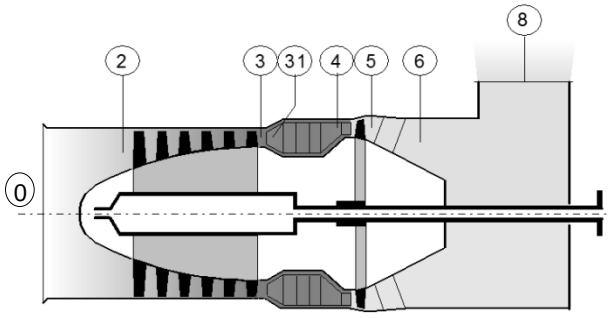

Station	Description
0	Ambient Surrounding / Air Inlet
2	Compressor Inlet
3	Compressor Outlet
31	Combustion Chamber Inlet (applied estimation: station 3 = station 31)
4	Combustion Chamber Outlet
5	Turbine Outlet
6	Exhaust Nozzle Cone Outlet
8	Exhaust Outlet to Ambient Surrounding

Figure 5: Station description of turbo shaft gas turbine [15]

The stations most important for the analysis presented in this work are:

- Station 0: measurement of the ambient surrounding air conditions pressure, temperature and humidity important for correction calculations of parameters to International Standard Atmosphere (ISA) conditions.
- Station 4: analysis of the combustion or turbine inlet conditions, respectively.
- Station 5: measurement of the exhaust gas conditions.

The required data for the analysis is obtained by several sensors. The ambient conditions pressure p_0, temperature T_0 and relative humidity of the surrounding air H_0 at the gas turbine air inlet are measured with an Ahlborn Almemo 8390-2 system. To determine the parameters in the combustion chamber at station 4, e.g. the combustion equivalence ratio Φ, exhaust gas samples are drawn for analysis. When sampling exhaust gases for chemical analysis, sophisticated considerations regarding extraction of the sample, design of the probe, heating of the probe and the tubing as far as the gas component analysing equipment are important to avoid concentration changes of the different components within the exhaust gas sample, condensation of water vapour in the tubing as well as condensation of unburned hydro-carbons influencing the analysis results. An appropriate sampling system design must consider typical conditions of the sampled gas, e.g. sample flow rate and velocity thereby influencing the probe and tubing size, condensation temperatures of typical exhaust gas components, pressure drop through the system etc. A proper

design of the sampling system ensures exhaust gas samples with representative concentrations of dissolved, suspended, and volatile constituents. To take into account all sampling requirements, the APU GTCP 36-300 test rig is equipped with a heated rotating isokinetic probe installed in the APU to extract representative isokinetic exhaust gas samples covering the complete flow area of the exhaust gas jet. The gas sample is directed to each analysing module by heated tubes and hoses under controlled pressure conditions in the ductwork. To analyse the sampled gas, a state-of-the-art exhaust gas analysing system from ABB is used determining the amount of unburned hydro carbons (C_xH_y analysed by ABB Multi FID 14) or of unburned hydrogen (H_2 analysed by ABB Caldos 27) respectively, the quantity of CO and CO_2 (analysed by ABB URAS 26) as well as the concentration of O_2 (analysed by ABB Magnos 206) in the exhaust gas. The total temperature T_{5t} at the turbine outlet is measured by the gas turbine thermocouples and an additional fast thermocouple connected to the test stand analysis system. The fuel mass flow of hydrogen and methane is obtained by a MicroMotion CMF050 mass flow meter and the power output of the APU is determined by an orifice measurement of the pneumatic bleed air output according to EN ISO 5167. A generator for electric power production is not installed in the APU. Since the bleed air power is directly proportional to the shaft power, it is used to determine the total gas turbine power output. The measuring devices and their measuring ranges and accuracies are summarized in Table 1.

Table 1: Description of analysis system devices, measuring ranges and accuracies

Device	**Component**	**Range**	**Accuracy**
Ahlborn Almemo 8390-2 Universal Measuring System	ambient pressure p_0	700 - 1050 mbar	± 0.5%
	ambient temperature T_0	0 - 70°C	± 0.1°C
	ambient humidity H_0	0 - 100 % r.H.	± 2% r.H.
ABB Multi FID 14	C_xH_y	0 - 25 000 ppm	≤ 2 %
ABB Caldos 27	H_2	0 - 4 Vol.%	≤ 2%
ABB URAS 26	CO	0 - 100 000 ppm	≤ 1 %
	CO_2	0 - 15 Vol.%	
ABB MAGNOS 206	O_2	0 - 50 Vol.%	≤ 0.5 %
div. thermocouples	relative temperature conditions	0 - 800 °C	± 0.25%
MicroMotion CMF050	fuel mass flow	1526 Nm³/h	± 0.35%

In Figure 6 the results from performance calculations and experimental analysis data is presented showing the required fuel mass flow for several load conditions (a) and the increase of temperature in the combustion chamber $(T_{4t}-T_{3t})$ (b) depicted versus the equivalence ratio Φ in the combustion chamber. In Figure 7 the corrected exhaust gas temperature at the turbine exit T_{5t} is depicted over the corrected shaft power output. All diagrams compare calculated data from the performance model with experimental data gathered by independent analysing systems (MicroMotion fuel meter, exhaust gas analysis system, restrictor measurement and thermocouple measurements). It can be observed that the measurement data and the GasTurb calculations show very good agreement and thereby validate the performance model of the APU for hydrogen and methane derived from the genuine kerosene model allowing detailed analyses of the gas turbine cycle further discussed in chapter 4.2.

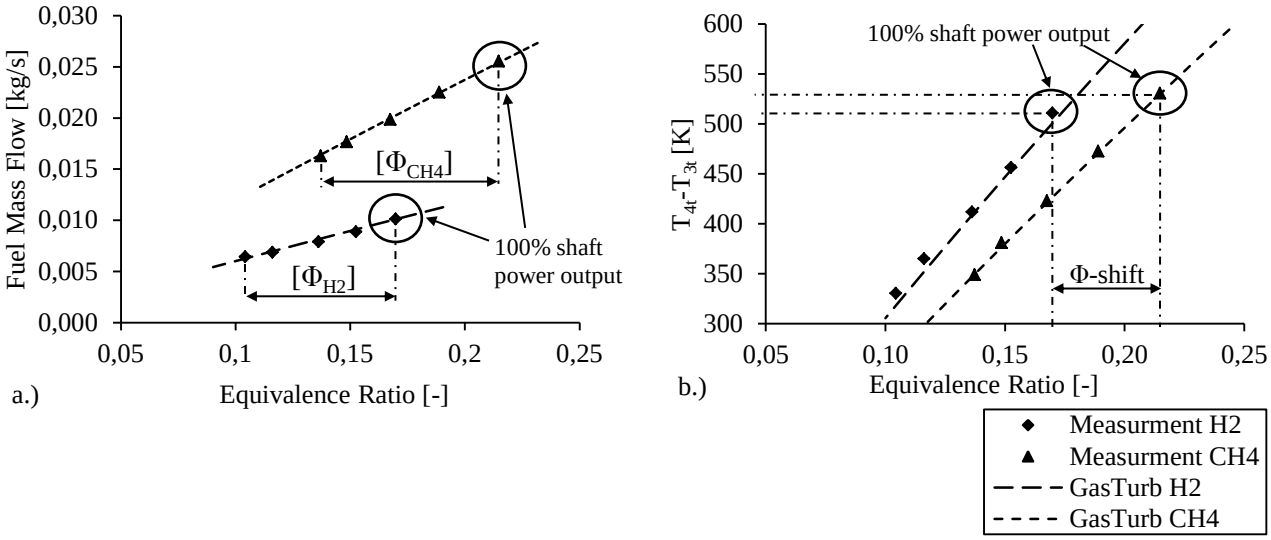

Figure 6: Fuel mass flow (a.) and temperature increase in the combustion chamber (b.)

Regarding Figure 7 there are always unconformities in the exhaust gas jet which cannot be covered by the applied temperature measuring method with equally distributed thermocouples on the exhaust circumference. To account for that, the grey shaded area in Figure 7 illustrates an unconformity scatter of the temperature distribution. It can be seen that in the higher power areas (80-100%), measurement and calculation are accurate while in the upper part load section (60%) the values are within the unconformity scatter; only in the low power area (< 40%) the measurement data is beyond the scatter. The performance model in GasTurb is validated for reliable manufacturer data for kerosene for high power operation. The part load section is extrapolated from the high power data and standard compressor and turbine maps implemented in GasTurb are used. In the relevant area of 80-100% power output discussed in this paper the model and the measuring data have a high reliability and reproducibility to allow profound analyses.

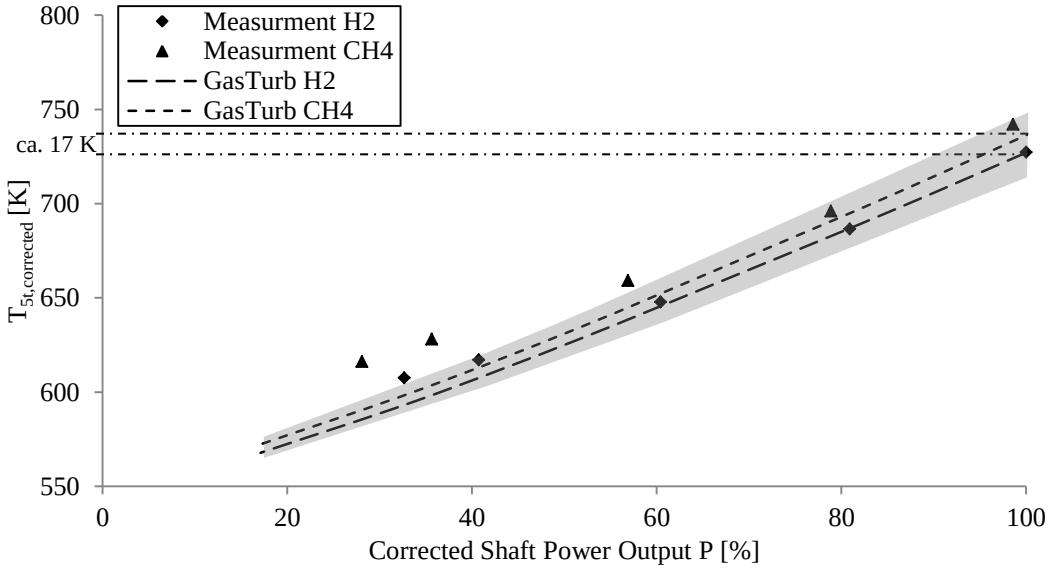

Figure 7: Corrected exhaust gas temperature

4.2 Influences on the Gas Turbine Cycle

In this section the thermodynamic cycle will be analysed in detail. Effects due to the application of the different fuels hydrogen and methane on the combustion equivalence ratio, the heat of combustion and subsequently the exhaust gas temperature as well as the influence on the operational behaviour of compressor, turbine and the complete gas turbine engine will be discussed.

Figure 6(b) highlights that changing from hydrogen to methane results in a shift of the equivalence ratio range in the gas turbine combustion chamber while maintaining the same shaft power output. Referring to equations (1) and (2), scaling with equal heat flow rate and therewith equal shaft power leads to a change in the required fuel mass flow and a subsequent shift in the equivalence ratio:

$$\Phi_{CH_4} = \Phi_{H_2} \cdot \frac{LHV_{H_2}}{LHV_{CH_4}} \cdot \frac{SAR_{CH_4}}{SAR_{H_2}} \quad (3).$$

Figure 6 also shows the shift to a more rich equivalence ratio range interval for methane resulting from the influence of the fuel lower heating value *LHV* and the impact of the stoichiometric air requirement *SAR* at similar heat flow rates and shaft power output. Since all relevant parameters are known (Table 2) the equivalence ratio shift can be calculated for the used fuels methane and hydrogen compared to kerosene:

$$\Phi_{fuel} = \frac{\dot{m}_{fuel} \cdot SAR_{fuel}}{\dot{m}_{air}} = \frac{\dot{Q}}{\dot{m}_{air}} \cdot \frac{SAR_{fuel}}{LHV_{fuel}} \quad (4)$$

In the case of the APU the coefficient ($\dot{Q}/\dot{m}_{air}$) can be considered as nearly constant, so the equivalence ratio is proportional to the ratio of the stoichiometric air requirement *SAR* divided by the lower heating value *LHV*:

$$\Phi \propto \frac{SAR_{fuel}}{LHV_{fuel}} \quad (5)$$

The determined ratios and the equivalence ratio shift of methane and hydrogen against kerosene are compared in Table 2. The result of the equivalence ratio shift shows, that the equivalence ratio of hydrogen is about 16.7% leaner compared to kerosene while methane remains in nearly identical order to kerosene, but is slightly richer.

Table 2: Properties of hydrogen, kerosene and methane, equivalence ratio shift relative to kerosene [16], [17], [18]

	Hydrogen H_2		**Kerosene Jet A-1**		**Methane CH_4**
SAR_{fuel} [kg_{Air}/kg_{fuel}]	34.3	>	14.7	<	17.2
LHV_{fuel} [MJ/kg]	119.95	>	42.80	<	50.03
$\frac{SAR_{fuel}}{LHV_{fuel}}$	0.2860	<	0.3435	<	0.3438
Φ-shift [-]	0.8326	<	1.0000	<	1.0009
Φ-shift [%]	- 16.74	<	0	<	+ 0.09

Observing Figure 7 it can be seen that between methane and hydrogen there is an off-set in the exhaust gas temperature. The exhaust gas temperature of methane is higher compared to the EGT of hydrogen by about 17 K at 100% shaft power. Comparing Figure 6 and Figure 7, the richer fuel mixture at methane operation and the leaner mixture at hydrogen operation resulting from the Φ-shift lead to different combustion temperatures changing the EGT on the turbine exit and surly will have effects on the operational point of the gas turbine.

In Figure 8 the compressor pressure ratio π_C versus the corrected shaft power output *P* is depicted for kerosene, methane and hydrogen. It can be observed that for a constant shaft power the pressure ratio of the compressor changes for different fuels. In Figure 8(b) the compressor characteristics are shown schematically for constant power. The APU GTCP 36-300 is a rotational speed controlled gas turbine running on constant 99% rotational speed for all ECS load conditions and on constant 101% speed in MES mode independent from the used fuel. The schematic presents that the operational point at constant power is shifted downwards along the line of operation with constant speed from kerosene over methane to hydrogen and show that the characteristics of the compressor, i.e. the compressor pressure ratio and the air mass flow through the compressor, must change. Two different effects must be considered regarding effects on the thermodynamic gas turbine cycle due to the changed operational point. (i) When the operational point of the gas turbine changes along the line of constant speed in the compressor map, the efficiency and the performance requirement of the turbine changes, too. Since the compressor pressure ratio π_C is influenced, the total efficiency η_t of the gas turbine cycle is also slightly affected, e.g. when π_C decreases, η_t

decreases. Simultaneously, the air mass flow $\dot{m}_{air}$ increases, resulting in a shift of the specific enthalpy ratios. The shift in the cycle operation point is influenced most by the change in combustion temperature T_{4t}.

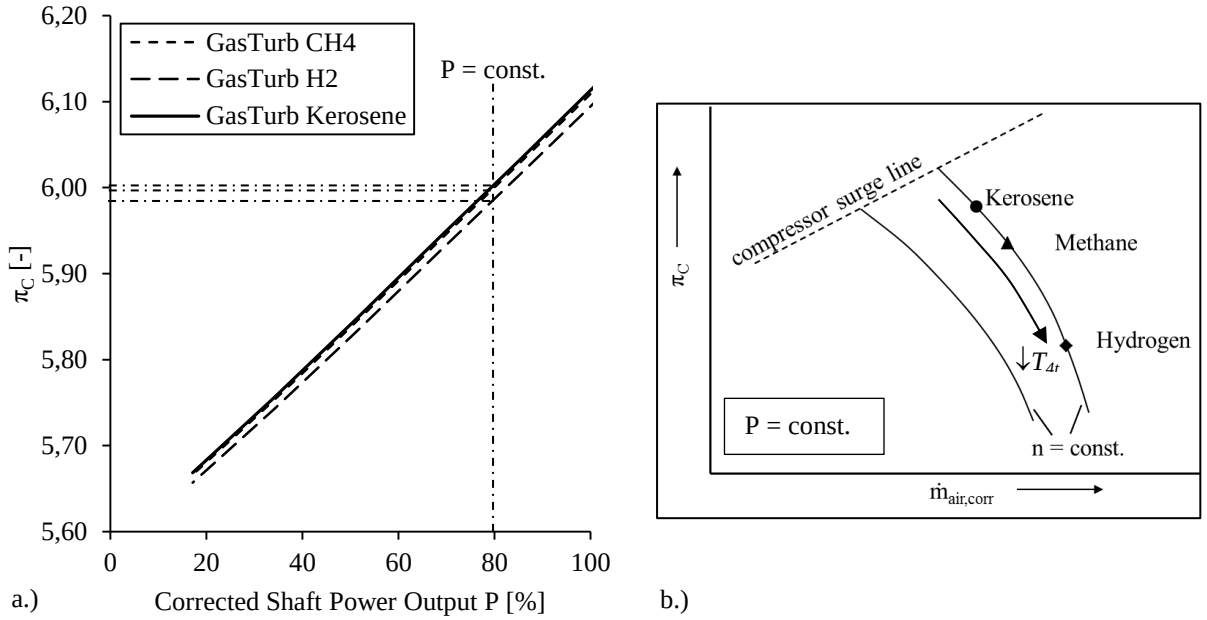

Figure 8: Compressor pressure ratio (a.), schematic compressor map (b.)

(ii) The cycle operational point is influenced by the different required fuel mass flows for kerosene, methane and hydrogen. The turbine power is reduced with decreasing fuel mass flow $\dot{m}_{fuel}$ and must be compensated in an increase in enthalpy Δh_T:

$$P_T \approx (\dot{m}_{air} + \dot{m}_{fuel}) \cdot \Delta h_T \tag{6}$$

Figure 8(b) shows that the shift along the operational line in the compressor map for hydrogen, methane and kerosene is influenced by the combustion temperature T_{4t}. Each kerosene, methane and hydrogen generates different combustion temperatures changing the operational point and the efficiency in the turbine. Generally, the influences on the efficiency of turbine and gas turbine cycle are minor, the interaction between T_{4t} and c_{pm} ($\bar{\bar{c}}_p$) are the dominant drivers for this phenomenon. The enthalpy in the turbine is

$$\Delta h_T \approx \bar{\bar{c}}_p \cdot T_{4_t} \cdot (1 - \tau) \tag{7}$$

Figure 9 points out the differences in the combustion temperature T_{4t}. In the figure the difference ΔT_{4t} between methane and kerosene and the difference between hydrogen and kerosene is presented calculated by GasTurb. At constant 100% power, T_{4t} of methane is about 7 K lower as the combustion temperature of kerosene. For hydrogen compared to kerosene the difference is even about 18 K lower matching the theory of Figure 8(b). In Figure 9(b) the combustion temperature T_{4t} is shown in relation to the equivalence ratio. Comparing the diagrams (a) and (b) it can be seen, that the differences of T_{4t} both of methane and hydrogen related to kerosene are not the same. Figure 9(a) shows the combustion temperature difference including the effect of the Φ-shift and the subsequent combustion temperature $T_{4t} = f(\Phi)$. In Figure 9(b) the temperature effect alone is depicted. It can be observed that at a constant equivalence ratio, hydrogen burns much hotter than methane. The Φ-shift leads to the effect that in the gas turbine in fact the hydrogen burns colder than kerosene and methane confirming the theory of Figure 8.
Regarding the T_{4t}-effect, a decrease leads to a lower turbine performance, but Figure 9(a) shows that 100% shaft power are maintained. Therefore, besides the combustion temperature, the impact of the mean isobaric heat capacity c_{pm} as well as the turbine temperature ratio $\tau = (T_{5t}/T_{4t})$ must be considered. Comparing the 100% shaft power output point in Figure 10 the diagram shows that τ of hydrogen is lower than the τ of methane. The mean isobaric heat capacity c_{pm} is depending on the equivalence ratio at the 100% power point. For hydrogen the c_{pm} at 100% power is higher than the c_{pm} of methane. So, For the hydrogen operation the higher c_{pm} combined with the reduced τ for hydrogen both have positive effects on the turbine enthalpy maintaining turbine power for 100% shaft power output together with a reduced fuel flow. It can be stated that for hydrogen the impact of τ and c_{pm} is dominant while for methane the T_{4t}-temperature effect is most significant.

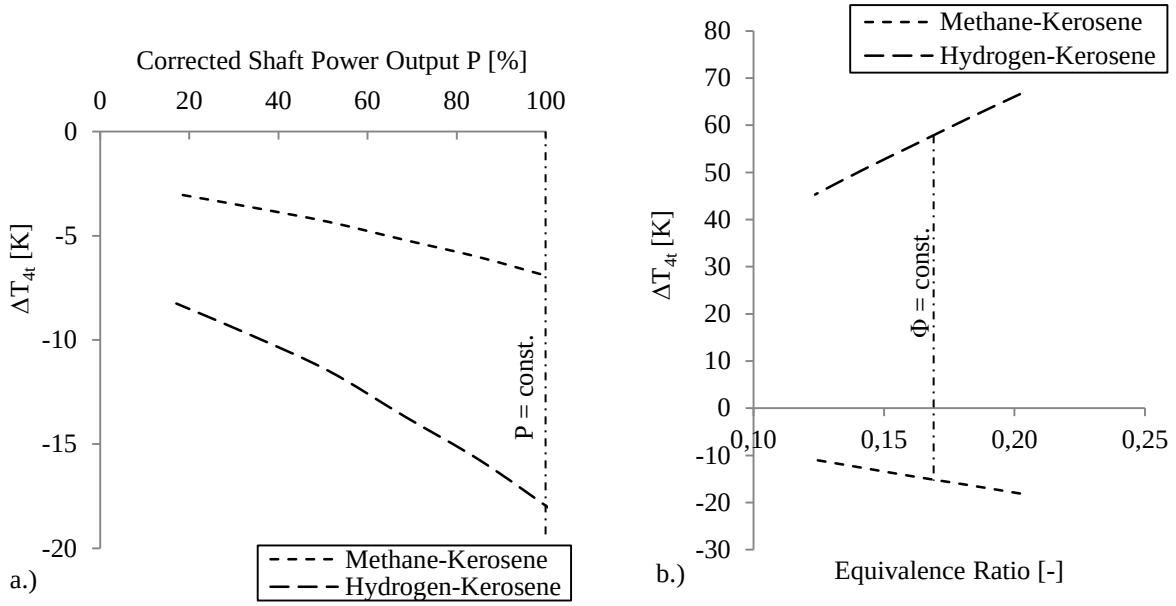

Figure 9: Combustion temperature difference related to kerosene calculated with GasTurb

In the case of τ another important effect must also be considered. Figure 9(a) shows that methane and hydrogen both have a lower combustion temperature compared to kerosene at constant power. As described earlier, the power of a gas turbine could be increased by scaling the combustion temperature (turbine inlet temperature) equal to kerosene generating more power and matching the same turbine inlet conditions. But as a result of the turbine temperature ratio characteristics τ it must be considered that therefore parts at the turbine exit are charged by higher temperatures as normal leading to life time reduction or even failure. Scaling to the same exhaust gas temperature T_{5t}, the effect remains the same, but the influence is different and while the parts at the turbine exit are normally charged, the area at the turbine inlet is affected by excessive heat. An increase in power of an existing gas turbine by the change of fuel with a higher heating value is possible, but sensitive considerations to avoid errors are important and modifications of the turbine cooling system should be taken into account.

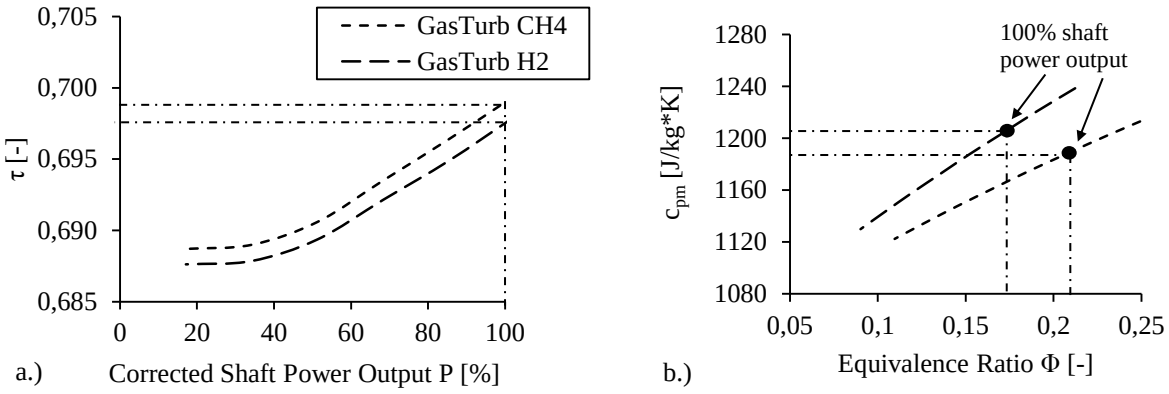

Figure 10: Turbine temperature ratio (a.) and isobaric heat capacity (b.)

The presented theoretical investigation of the gas turbine cycle supported by GasTurb calculations shows that the change of fuel has significant impact on the gas turbine and influences the designed operation point depending on which fuel is used. The fuel properties of kerosene, methane and hydrogen influence the fuel-air-mixture in the combustion chamber and lead to an equivalence ratio shift and differing combustion temperatures. This affects the operational point of the gas turbine at constant power because the compressor characteristics and turbine performance are changed. The balance between the combustion temperature, the mean isobaric heat capacity and the turbine temperature ratio significantly influence turbine power and also the exhaust gas temperature level. This again

has an impact on the control strategy of the gas turbine on the one hand and offering on the other hand the benefit of possible increased gas turbine power switching from kerosene to methane and hydrogen.

5. Conclusion

The presented work shows that it is possible that a gas turbine converted to the use of gaseous fuels can be run alternatively with hydrogen and methane. For this alternating operation no mechanical changes of the gas turbine for gaseous fuels is required, only slight modifications of the gas turbine start-up-controller software are necessary regarding the ignition and initial acceleration process of the gas turbine. In a future scope of work the gas turbine main engine controller can be optimized by improving the on-speed-governor for the dual-fuel operation with hydrogen and methane implementing adaptable control parameters when switching between fuels.
The theoretical investigation of the gas turbine cycle supported by GasTurb calculations shows that the change of fuel has a significant impact on the gas turbine operation point depending on which fuel is used. The fuel properties of kerosene, methane and hydrogen influence the fuel-air-mixture in the combustion chamber and lead to an equivalence ratio shift and differing combustion temperatures. This affects the operational point of the gas turbine at constant power because the compressor characteristics and turbine performance are changed. The balance between the combustion temperature, the isobaric heat capacity and the turbine temperature ratio significantly influences the turbine power and also the exhaust gas temperature level. This again has an impact on the control strategy of the gas turbine, but also offering the benefit of possible increased gas turbine power. Maintaining the same exhaust gas temperature for kerosene or methane, hydrogen offers the opportunity to increase the power output of an existing gas turbine, but the influences of the different behaviour in the turbine temperature ratio must be considered to avoid overheating of turbine parts. Another interesting aspect is, when changing a gas turbine from kerosene or methane to hydrogen, fuel consumption is significantly reduced and the hydrogen burning colder at the same power output level offers the opportunity to increase the turbine section hot parts life time because the prevailing temperatures at the turbine inlet are reduced.

6. Nomenclature

Abbreviations

APU	auxiliary power unit	O_2	oxygen
CH_4	Methane	P	power
CO	carbon monoxide	p	pressure
CO_2	carbon dioxide	$\dot{Q}$	heat flow rate
c_{pm}, $\bar{\bar{c}}_p$	mean isobaric heat capacity	SAR	stoichiometric air requirement
ECS	environmental control supply	T	temperature
H_2	hydrogen	Δt	time index difference
H	humidity	UH	unburned hydrogen
h	enthalpy	UHC	unburned hydro-carbons (C_xH_y)
IGV	inlet guide vanes	VECB	versatile engine control box
LHV	lower heating value	η_T	total efficiency
$\dot{m}$	mass flow rate	Φ	equivalence ratio
MES	main engine start	π_C	compressor pressure ratio
N_2	Nitrogen	τ	turbine temperature ratio

Subscriptions

0	station 0	3	station 3
4	station 4	5	station 5
Air	air-related	corr	corrected
Fuel	fuel-related	T	turbine
t	Total		

7. References

[1] Lieuwen, T., Yang, V., Yetter, R. 2010. Synthesis Gas Combustion: Fundamentals and Applications. Published by CRC Press Taylor & Francis Group.

[2] Dahl, G., Suttrop, F. 1998. Engine Control and Low-NO_x Combustion for Hydrogen Fuelled Aircraft Gas Turbines. In: *Int. J. Hydrogen Energy*. 23:695-704.

[3] Suttrop, F., Dorneiski, R. 1991. Low NO_x-Potential of Hydrogen-Fuelled Gas Turbine Engines. In: *1st Int. Conference on Comb. Techn. for Clean Environment*.

[4] Funke, H. H.-W., Börner, S., Hendrick, P., Recker, E. 2009. Modification and testing of an engine and fuel control system for a hydrogen fuelled gas turbine. In: *3rd European Conference for Aeronautics and Space Sciences (EUCASS).* Published in: *Progress in Propulsion Physics Vol. III*.

[5] Funke, H. H.-W., Börner, S., Hendrick, P., Recker E. 2010. Control System Modifications for a Hydrogen Fuelled Gas-Turbine. In: *13th International Symposium on Transport Phenomena and Dynamics of Rotating Machinery (ISROMAC13)*

[6] Funke, H. H.-W., Börner, S., Hendrick, P., Recker, E., Elsing, R. 2011. Development and integration of a scalable low NO_x combustion chamber for a hydrogen fuelled aero gas turbine. In: 4th *European Conference for Aeronautics and Space Sciences (EUCASS).* Accepted for: *Advances in Propulsion Physics*.

[7] Börner, S., Funke, H. H.-W., Falk, F., Hendrick, P. 2011. Control system modifications and their effects on the operation of a hydrogen-fueled Auxiliary Power Unit. In: *20th International Symposium on Air Breathing Engines (ISABE 2011)*.

[8] Westfalen AG. 2010. Hydrogen – Safety Data Sheet.

[9] Westfalen AG. 2010. Methane – Safety Data Sheet.

[10] Chiesa, P., Lozza, G., Mazzocchi, L. 2005. Using Hydrogen as Gas Turbine Fuel. In: *Journal of Engineering for Gas Turbines and Power, Vol. 127, Transactions of the ASME*.

[11] Verstraete, D., Hendrick, P., Pilidis, P., Ramsden, K. 2005. Hydrogen as an (Aero) Gas Turbine Fuel. In: *17th International Symposium on Air Breathing Engines (ISABE 2005)*.

[12] Kurzke, J. 2005. How to Create a Performance Model of a Gas Turbine from a Limited Amount of Information. In: *Proceedings of the ASME Turbo Expo 2005: Power for Land, Sea and Air*.

[13] Kurzke, J. 1996. How to Get Component Maps for Aircraft Gas Turbine Performance Calculations. In: *Proceedings of the International Gas Turbine and Aeroengine Congress & Exhibition of the American Society of Mechanical Engineering*.

[14] Kurzke, J. 2003. Model Based Gas Turbine Parameter Corrections. In: *Proceedings of the ASME Turbo Expo 2003: Power for Land, Sea and Air*.

[15] Kurzke, J. 2012. GasTurb – Design and Off-Design Performance of Gas Turbines. Software-Manual.

[16] Esch. Th. 2011. Combustion Technology. Aachen University of Applied Sciences.

[17] Deutsches Institut für Normung e.V. 1997. Berechnung von Brennwert, Heizwert, Dichte, relativer Dichte und Wobbeindex von Gasen und Gasgemischen. In: *DIN 51857:1997-03*.

[18] Exxon Mobil Aviation. 2008. World Jet Fuel Specifications.